2008 IEEE/RSJ International Conference on Intelligent Robots and Systems
Acropolis Convention Center
Nice, France, Sept, 22-26, 2008

Calibration and On-line Data Selection of Multiple Optical Flow Sensors for Mobile Robot Localization

Jwu-Sheng Hu, Yung-Jung Chang, and Yu-Lun Hsu

Abstract— **This paper proposes a calibration method as well as a computational algorithm to integrate the data of multiple optical flow sensors for 2-dimensional trajectory measurement. Optical flow sensors offer a different kind of odometer as compared with the wheel encoder. Using multiple sensors, it is possible to reduce the effect of measurement uncertainties. Since all sensors are mounted on a rigid body, their measurement data must obey a certain relation. This relation is utilized in this paper and mathematical formulations are developed to realize the computation. It is shown that the calibration procedure can be cast as an optimization problem given measurement data. Further, the rigid-body relation is formulated as a null-space constraint using the calibrated parameters. During operation, unreliable sensor measurements can be removed by accessing the error distance to the null space. Experimental results are presented to support the proposed methods.**

I. Introduction

LOCALIZING a mobile robot in an indoor environment is an important issue in the field of robotics. The position estimation methods can be classified into two basic categories: absolute and relative positioning [1]. Common absolute positioning technologies include GSP, navigation beacons, map-matching and landmarks and for relative positioning, odometers or inertial sensors are usually used. Localization integrating various sensors is a clever way to complement the drawbacks of individual sensor. However, improving the accuracy of one kind of sensor is fundamental to enhance the accuracy of localization.

Odometer based on wheel encoder is most commonly used in practice because of its simplicity and availability. Recently, the method of localization using optical flow sensors (or optical mouse sensor) was proposed [3]–[10]. Combining the measurement with landmarks to perform self-localization was also reported [6][11]. Comparing to optical encoder, the optical flow sensor measurement is not affected by wheel-slippage because of direct sensing of the movement between the sensor and sensing surface. Further, the cost of the sensor is very low due to its massive applications of computer mice. It is now easy to obtain off-the-shelf optical flow sensor whose resolution reaches 2000 counts per inch.

The principle of optical mouse is using a miniaturized CMOS camera to capture consecutive images reflected from the surface through the LED illumination. The camera, LED and associated optical mechanism are specially arranged to ensure a robust measurement [9]. Because the surface has texture variation, it is then likely to detect the motion of the sensor by matching the patterns between consecutive images (e.g., autocorrelation [12]). Although it is possible to obtain both translational and rotational measurement, off-the-shelf sensors only give translation information because rotation is not needed in computer mouse applications. Therefore, at least two optical flow sensors have to be used to detect the complete motion information [4]–[5] [7]–[8].

There are many factors that might affect the accuracy of the optical flow measurement. The work in [9] provides a detailed analysis of the possible errors of the optical flow sensor itself and it is possible to reduce the error by taking average over an array of sensors. However, taking the average does not consider the differences among the sensors as they might encounter different conditions. For example, the optical flow sensor passing by a hole (i.e., a sudden change of height of the surface) gives an incorrect reading due to out-of-focus. Further, to use multiple sensors, there are more issues to be considered. Borenstein and Feng [2] categorized the errors into: 1) Systematic errors and 2) Non-systematic errors. For our case, the reasons leading to the systematic error include imperfect measurements of position and orientation of optical flow sensors and variation of resolutions. The reasons of the non-systematic error come from the sensor itself such as inability to detect the change of a homogeneous surface or the distance between sensor and sensing surface is too large [7].

The technical issues mentioned above have never been studied in detail when constructing a sensor module using multiple optical flow sensors. This work proposes a calibration method to deal with the systematic errors as well as a consistency check strategy to reduce the inaccuracy affected by non-systematic errors. The underlying principle is similar to sensor fusion where the readings of all sensors must reflect the fact that they are mounted under a rigid body. Rigorous mathematical formulations and derivations are given to facilitate the design in real practice. The following section describes the methods of integrating multiple optical flow sensors. In section III, the rigid-body constraints and the geometric relations of optical flow sensors are introduced. Section IV presents the calibration method which optimizes

Manuscript received February 22, 2008. This work was supported in part by the National Science Council of Taiwan, ROC under grant NSC 95-2221-E-009-177- and the Ministry of Economic Affairs under grant 95-EC-17-A-04-S1-054.

J. S. Hu, Y. J. Chang, and Y. L. Hsu are with Department of Electrical and Control Engineering, National Chiao Tung University, Hsinchu 300, Taiwan, ROC. (e-mail: jshu@cn.nctu.edu.tw; nuo.ece95g@nctu.edu.tw; lun.ece96g@nctu.edu.tw).

the parameters of sensors using the formulation in section III. In Section V, the consistency check strategy is developed to choose the reliable sensor measurements during operation. Several simulation results are given in Section VI to demonstrate the proposed method and a conclusion is given in Section VII.

II. Position and Orientation Estimation Using Multiple Sensors

The analysis in this section makes an extension of the work in [7] to multiple sensors. Consider there are N optical flow sensors, labeled as i = 1 to N, mounted on a plane. Each sensor is able to measure a 2-dimensional translation in its own coordinate. In general, sensor coordinates (coordinate defined on the motion detection axes of the optical flow sensor) are not necessary aligned to each other. Suppose two sensors labeled i and j (Fig. 1) are at a distance D_{ij} to each other. The coordinate of sensor i is rotated at the angle σ_{ij} relative to the line connecting both sensors (line $\overline{O_iO_j}$ in Fig. 1) while the angle for sensor j is σ_{ji}. The sign of σ_{ij} and σ_{ji} is positive if the rotation is counterclockwise (CCW) and negative otherwise.

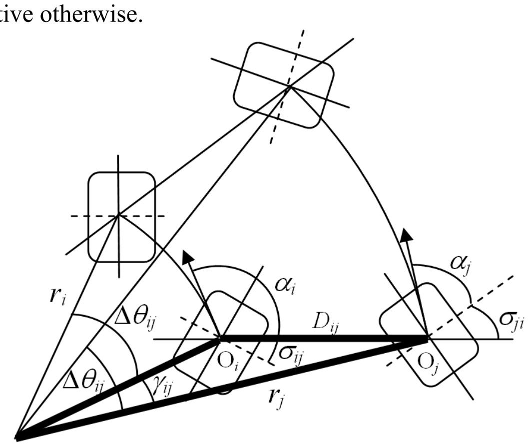

Fig. 1. Geometric relation of two sensors

Considering that the sensor move along an arc during the sampling interval, the length of the arc is,

$$l_i = \sqrt{\bar{x}_i^2 + \bar{y}_i^2} \tag{1}$$

where $\bar{x}_i$ and $\bar{y}_i$ are the measurements of sensor i at each sample instant on the coordinate of sensor i. The motion direction (tangent to the arc) of sensor i is at the angle α_i relative to the sensor coordinate, i.e.

$$l_i \cos(\alpha_i) = \bar{x}_i \text{ and } l_i \sin(\alpha_i) = \bar{y}_i . \tag{2}$$

From Fig. 1, the angle γ_{ij} can be calculated as $\gamma_{ij} = |\alpha_i + \sigma_{ij} - \alpha_j - \sigma_{ji}|$. Denoting the rotational angle as $\Delta\theta_{ij}$, the radius of rotation for sensor i is,

$$r_i = \frac{l_i}{\Delta\theta_{ij}} \tag{3}$$

and from the law of cosine, $\Delta\theta_{ij}$ can be calculated as,

$$\Delta\theta_{ij} = \frac{\sqrt{l_i^2 + l_j^2 - 2\cos(\gamma_{ij}) l_i l_j}}{D_{ij}} sign(l_j \sin(\alpha_j + \sigma_{ij}) - l_i \sin(\alpha_i + \sigma_{ij})) \tag{4}$$

Define a coordinate (x', y') aligned with the line $\overline{O_iO_j}$ and the origin located at its mid-point (Fig. 2). The new sensor locations can be calculated as,

$$x_i' = r_i(\sin(\Delta\theta_{ij} + \alpha_i + \sigma_{ij}) - \sin(\alpha_i + \sigma_{ij}))sign(\Delta\theta_{ij}) + D_{ij}/2 \tag{5a}$$

$$y_i' = r_i(\cos(\alpha_i + \sigma_{ij}) - \cos(\Delta\theta_{ij} + \alpha_i + \sigma_{ij}))sign(\Delta\theta_{ij}) \tag{5b}$$

$$x_j' = r_j(\sin(\Delta\theta_{ij} + \alpha_j + \sigma_{ji}) - \sin(\alpha_j + \sigma_{ji}))sign(\Delta\theta_{ij}) - D_{ij}/2 \tag{5c}$$

$$y_j' = r_j(\cos(\alpha_j + \sigma_{ji}) - \cos(\Delta\theta_{ij} + \alpha_j + \sigma_{ji}))sign(\Delta\theta_{ij}) \tag{5d}$$

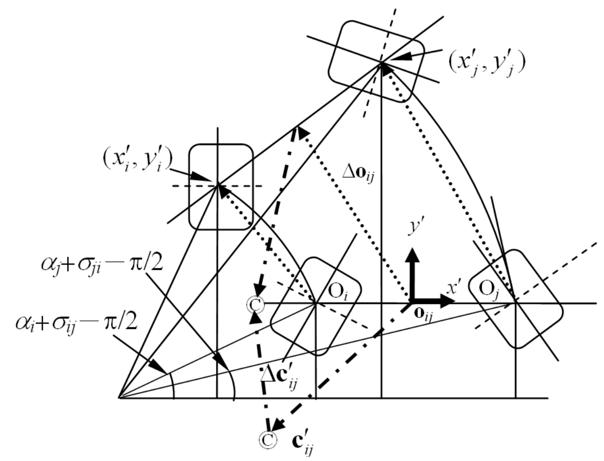

Fig. 2. The movement within a sampling interval of two sensors

Denoting the center of the line $\overline{O_iO_j}$ as $\mathbf{o}_{ij}$ and its movement as $\Delta\mathbf{o}_{ij}$ (see Fig. 2), we have,

$$\Delta\mathbf{o}_{ij} = \begin{bmatrix} \Delta x_{ij}' & \Delta y_{ij}' \end{bmatrix}^T \tag{6}$$

where

$$\Delta x_{ij}' = {(x_i' + x_j')}/{2} \text{ and } \Delta y_{ij}' = {(y_i' + y_j')}/{2} .$$

Suppose that the center of the robot relative to the $\mathbf{o}_{ij}$ on the coordinate of Fig. 2 is $\mathbf{c}_{ij}'$, the movement of the center, denoted as $\Delta\mathbf{c}_{ij}'$, is

$$\Delta\mathbf{c}_{ij}' = (\mathbf{T}(\Delta\theta_{ij}) - \mathbf{I})\mathbf{c}_{ij}' + \Delta\mathbf{o}_{ij} \tag{7}$$

where $\mathbf{I}$ is the identity matrix and $\mathbf{T}(\Delta\theta_{ij})$ is the transformation matrix as,

$$\mathbf{T}(\Delta\theta_{ij}) = \begin{bmatrix} \cos(\Delta\theta_{ij}) & -\sin(\Delta\theta_{ij}) \\ \sin(\Delta\theta_{ij}) & \cos(\Delta\theta_{ij}) \end{bmatrix} \tag{8}$$

Suppose the orientation of the vector $\overrightarrow{O_iO_j}$ to the robot coordinate is β_{ij}, the movement represented by the robot coordinate (denoted as $\Delta\mathbf{c}_{ij}$) is

$$\Delta\mathbf{c}_{ij} = \mathbf{T}(\beta_{ij})\Delta\mathbf{c}_{ij}' \tag{9}$$

Therefore, the robot position and orientation relative to the global coordinate computed from the sensor pair i and j at time k+1 are,

$$\theta(k+1) = \theta(k) + \Delta\theta_{ij} \tag{10}$$

$$\mathbf{c}(k+1)=\mathbf{c}(k)+\mathbf{T}(\theta(k))\Delta\mathbf{c}_{ij} \tag{11}$$

For N sensors, there will be $C_2^N=N(N\text{-}1)/2$ solutions for the robot position and orientation update. A straightforward way of update is to compute the mean as,

$$\theta(k+1)=\theta(k)+\frac{2}{N(N-1)}\sum_{i=1}^{N-1}\sum_{j=i+1}^{N}\Delta\theta_{ij} \tag{12}$$

$$\mathbf{c}(k+1)=\mathbf{c}(k)+\frac{2}{N(N-1)}\mathbf{T}(\theta(k))\sum_{i=1}^{N-1}\sum_{j=i+1}^{N}\Delta\mathbf{c}_{ij} \tag{13}$$

III. The Rigid-body Constraints and Geometric Relations among Sensors

Since all sensors are fixed relative to each other, the measurements must obey the rigid body constraint. This constraint can be used to perform calibration as well as access the correctness of measurement. For rigid body motion, the constraint between any two sensors according to Fig. 1 is

$$l_i\cos(\alpha_i+\sigma_{ij}) = l_j\cos(\alpha_j+\sigma_{ji}) \tag{14}$$

or

$$l_i\cos(\alpha_i)\cos(\sigma_{ij})- l_i\sin(\alpha_i)\sin(\sigma_{ij}) = l_j\cos(\alpha_j)\cos(\sigma_{ji})- l_j\sin(\alpha_j)\sin(\sigma_{ji}). \tag{15}$$

This means that the projections of the sensor measurements onto the joining line in Fig. 1 should be the same. For N sensors, there will be $N(N\text{-}1)/2$ constraint equations. Since $l_i\cos(\alpha_i) = \overline{x}_i$ and $l_i\sin(\alpha_i) = \overline{y}_i$, where $\overline{x}_i$ and $\overline{y}_i$ are the sensor measurements during each sampling interval on the sensor coordinate. The equation becomes

$$\overline{x}_i\cos(\sigma_{ij})-\overline{y}_i\sin(\sigma_{ij})= \overline{x}_j\cos(\sigma_{ji})-\overline{y}_j\sin(\sigma_{ji}) \tag{16}$$

and the equation error is defined as

$$\varepsilon_{ij} = \overline{x}_i\cos(\sigma_{ij})-\overline{y}_i\sin(\sigma_{ij})-\overline{x}_j\cos(\sigma_{ji})+\overline{y}_j\sin(\sigma_{ji}) \tag{17}$$

The pattern ε_{ij} of can be used to access if the nominal parameters is correct or if the sensor reading is reliable. Define the error vector $\boldsymbol{\varepsilon}$ as the collection of $N(N\text{-}1)/2$ errors ε_{ij},

$$\boldsymbol{\varepsilon}=\begin{bmatrix}\varepsilon_{12} & \varepsilon_{13} & \cdots & \varepsilon_{(N-1)N}\end{bmatrix}^T=\mathbf{B}\cdot X \tag{18}$$

where $\mathbf{B}$ is a matrix of dimension $N(N\text{-}1)/2\times 2N$ shown in (19) at the bottom of this page. X is defined as sensor measurements vector as $X=[\overline{x}_1\ \ \overline{y}_1\ \ \overline{x}_2\ \ \overline{y}_2\ \ \cdots\ \ \overline{x}_N\ \ \overline{y}_N]^T$ whose dimension is $2N\times 1$. Moreover, denoting the orientation of the sensor i to the robot coordinate is ϕ_i and for sensor j is ϕ_j, the angle σ_{ij} can be obtained from $\sigma_{ij} = \phi_i-\beta_{ij}$ and similarly, $\sigma_{ji} = \phi_j-\beta_{ij}$.

Equation (18) can be used to compute the parameters in $\mathbf{B}$ by minimizing $\boldsymbol{\varepsilon}$. $\mathbf{B}$ contains the angular parameters of sensors, i.e. all ϕ_i's and β_{ij}'s. The number of ϕ_i is N and the number of β_{ij} is $N(N\text{-}1)/2$ (since $\beta_{ji} = \beta_{ij} + \pi$ and there are no β_{ii}'s). However, all ϕ_i's are independent to each other but β_{ij}'s are not. In other words, there are relations among β_{ij}'s which should be satisfied when performing the minimization to find the parameters. To begin with, define the coordinate of sensor 1 as the robot coordinate and the center of sensor 1 as the robot center, i.e. $\phi_1 = 0$ and the position of sensor 1 is (0,0). Fig. 3 shows the relations among sensor number 1, i, i+1, j and j-1. There are two cases when computing β_{ij}.

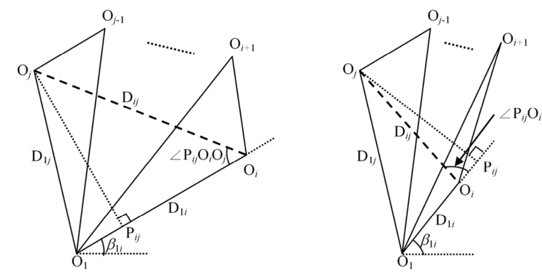

(a) (b)

Fig. 3. The geometric relations of angles: (a) acute angle case. (b) obtuse angle case

In Fig.3, suppose that $\overline{\mathrm{P}_{ij}\mathrm{O}_i}$ is perpendicular to $\overline{\mathrm{O}_i\mathrm{O}_j}$ and the point P_{ij} is a point on line $\overline{\mathrm{O}_i\mathrm{O}_j}$. In the first case (Fig.3(a)), $\angle\mathrm{P}_{ij}\mathrm{O}_i\mathrm{O}_j$ is an acute angle and it is easy to see that the angle $\beta_{ij} = \beta_{1i} + (\pi-\angle\mathrm{P}_{ij}\mathrm{O}_i\mathrm{O}_j)$. Let $\psi_{a,b,c}$ be the notation of angle $\angle\mathrm{O}_a\mathrm{O}_b\mathrm{O}_c$. and D_{ij} the length of $\overline{\mathrm{O}_i\mathrm{O}_j}$. We can see that the length of $\overline{\mathrm{P}_{ij}\mathrm{O}_j}$ is equal to $\mathrm{D}_{1j}\sin(\psi_{i,1,j})$ and the length of $\overline{\mathrm{P}_{ij}\mathrm{O}_i}$ is equal to $\mathrm{D}_{1i}-\mathrm{D}_{1j}\cos(\psi_{i,1,j})$. As a result, the angle $\angle\mathrm{P}_{ij}\mathrm{O}_i\mathrm{O}_j$ is

$$\angle\mathrm{P}_{ij}\mathrm{O}_i\mathrm{O}_j=\arctan\left(\frac{D_{1j}\sin(\psi_{i,1,j})}{D_{1i}-D_{1j}\cos(\psi_{i,1,j})}\right) \tag{20}$$

and according to law of cosine,

$$D_{1i}=\frac{\sin(\psi_{1,i+1,i})\sin(\psi_{1,i+2,i+1})\cdots\sin(\psi_{1,j,j-1})}{\sin(\psi_{1,i,i+1})\sin(\psi_{1,i+1,i+2})\cdots\sin(\psi_{1,j-1,j})}D_{1j} \tag{21}$$

Hence,

$$\angle P_{ij}O_iO_j=\arctan\left(\frac{\sin(\psi_{i,1,j})}{\dfrac{\sin(\psi_{1,i+1,i})\sin(\psi_{1,i+2,i+1})\cdots\sin(\psi_{1,j,j-1})}{\sin(\psi_{1,i,i+1})\sin(\psi_{1,i+1,i+2})\cdots\sin(\psi_{1,j-1,j})}-\cos(\psi_{i,1,j})}\right) \tag{22}$$

In the second case (Fig.3(b)), the angle $\angle\mathrm{P}_{ij}\mathrm{O}_i\mathrm{O}_j$ is an obtuse angle and $\beta_{ij}= \beta_{1i} + \angle\mathrm{P}_{ij}\mathrm{O}_i\mathrm{O}_j$. Similarly, we can arrive at the following equation.

$$\boldsymbol{B}=\begin{bmatrix}\cos(\sigma_{12}) & -\sin(\sigma_{12}) & -\cos(\sigma_{21}) & \sin(\sigma_{21}) & 0 & 0 & \cdots & \cdots & \cdots & \cdots & 0\\ \cos(\sigma_{13}) & -\sin(\sigma_{13}) & 0 & 0 & -\cos(\sigma_{31}) & \sin(\sigma_{31}) & \cdots & \cdots & \cdots & \cdots & 0\\ \vdots & \vdots & \vdots & \vdots & \vdots & \vdots & \vdots & \vdots & \vdots & \vdots & \vdots\\ 0 & 0 & 0 & 0 & 0 & 0 & \cdots & \cos(\sigma_{(N-1)N}) & -\sin(\sigma_{(N-1)N}) & -\cos(\sigma_{N(N-1)}) & \sin(\sigma_{N(N-1)})\end{bmatrix} \tag{19}$$

$$\angle P_{ij}O_iO_j = \arctan\left(\frac{\sin(\psi_{i,1,j})}{\cos(\psi_{i,1,j}) - \frac{\sin(\psi_{1,i+1,i})\sin(\psi_{1,i+2,i+1})\cdots\sin(\psi_{1,j,j-1})}{\sin(\psi_{1,i,i+1})\sin(\psi_{1,i+1,i+2})\cdots\sin(\psi_{1,j-1,j})}}\right) \quad (23)$$

Further, it is straightforward to show that that $\psi_{i,1,j} = \beta_{1j} - \beta_{1i}$, $\psi_{1,i,i+1} = \pi - (\beta_{ii+1} - \beta_{1i})$, $\psi_{1,i+1,i} = \beta_{ii+1} - \beta_{1i+1}$, $\psi_{1,i+1,i+2} = \beta_{i+1i+2} - \beta_{1i+1}$, $\psi_{1,i+2,i+1} = \pi - (\beta_{i+1\ i+2} - \beta_{1\ i+2})$, and so on. Therefore, the angle β_{ij} can be rewritten as,

$$\beta_{ij} = \begin{cases} \beta_{1i} + \pi - \arctan\left(\dfrac{\sin(\beta_{1j} - \beta_{1i})}{S_{ij} - \cos(\beta_{1j} - \beta_{1i})}\right), & \text{case (a)} \\ \beta_{1i} + \arctan\left(\dfrac{\sin(\beta_{1j} - \beta_{1i})}{\cos(\beta_{1j} - \beta_{1i}) - S_{ij}}\right), & \text{case (b)} \end{cases} \quad (24)$$

where

$$S_{ij} = \frac{\sin(\beta_{i\ i+1} - \beta_{1\ i+1})\sin(\beta_{i+1\ i+2} - \beta_{1\ i+2})\cdots\sin(\beta_{j-1\ j} - \beta_{1\ j})}{\sin(\beta_{i\ i+1} - \beta_{1\ i})\sin(\beta_{i+1\ i+2} - \beta_{1\ i+1})\cdots\sin(\beta_{j-1\ j} - \beta_{1\ j-1})}$$

Equation (24) shows the relationship among β_{ij}'s and it is easy to see that the free parameters are β_{1j}'s, j = 2 to N and $\beta_{i(i+1)}$'s, i=2 to N-1. All other β_{ij}'s can be computed from them using (24).

Given the angle β_{ij}'s, there are also geometry relations among D_{ij}'s. In fact, there is only one degree of freedom left for D_{ij}'s. To see this, consider the geometric relations shown in Fig. 4 and according to law of cosine,

$$D_{1j} = \frac{\sin(\psi_{1,2,j})}{\sin(\psi_{1,j,2})} D_{12} \quad . \quad (25)$$

Then,

$$D_{ij} = \frac{\sin(\psi_{i,1,j})}{\sin(\psi_{1,i,j})} D_{lj} = \frac{\sin(\psi_{i,1,j})\sin(\psi_{1,2,j})}{\sin(\psi_{1,i,j})\sin(\psi_{1,j,2})} D_{l2} \quad (26)$$

Equivalently, we can have

$$D_{ij} = G_{ij} \cdot D_{12} \quad (27)$$

where

$$G_{ij} = \begin{cases} \dfrac{\sin(\beta_{2j} - \beta_{12})}{\sin(\beta_{2j} - \beta_{1j})} & \text{, when } i = 1 \\ \dfrac{\sin(\beta_{1j} - \beta_{1i})\sin(\beta_{2j} - \beta_{12})}{\sin(\beta_{ij} - \beta_{1i})\sin(\beta_{2j} - \beta_{1j})} & \text{, otherwise} \end{cases}$$

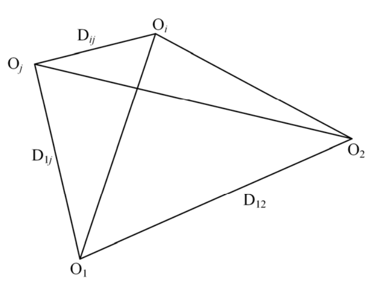

Fig. 4. Geometric relations of D_{ij}

As the result, the position of each sensor relative to sensor 1 can derive from D_{12} and β_{ij}. These geographic relations are fundamental to the calibration as well as consistency check algorithm described in the following context.

IV. The Calibration Method

The objective of calibration is to reduce the systematic errors by correcting parameters of the sensor configuration. Using (18) and (24), one can determine the angular parameters (ϕ_i's and β_{ij}'s) and subsequently, the distance among sensors can be computed from (27) given one distance measurement between a pair of sensors. In other words, if that distance measurement and all sensor readings are accurate, it is able to perform self-calibration without using external reference measurements. Suppose measurements obtained by moving the sensor module in a homogeneous path (e.g. an arc or a line) for a while are accumulated and the accumulated data set is denoted as the following vector,

$$X = \begin{bmatrix} \bar{x}_1 & \bar{y}_1 & \bar{x}_2 & \bar{y}_2 & \cdots & \bar{x}_N & \bar{y}_N \end{bmatrix}^T \quad (28)$$

Instead of using one sample data, using accumulated data could prevent quantization error. The trajectory of sensor motion shall be designed such that the vector X spans the remaining subspace (a condition similar to persistence excitation).

As described in Section III, the independent angular parameters are ϕ_i's, i=2 to N, β_{1j}'s, j=2 to N and $\beta_{k(k+1)}$'s, k=2 to N-1. The total number is (N–1)+(N–1)+(N–2)=3N–4. Let Z be the vector $Z = [z_1\ z_2\ \ldots\ z_{3N-4}]^T = [\phi_2\ \ldots\ \phi_N\ \beta_{12}\ \beta_{13}\ \ldots\ \beta_{1N}\ \beta_{23}\ \beta_{34}\ \ldots\ \beta_{(N-1)N}]^T$. The problem of solving Z can be cast as the following optimization problem,

$$\underset{Z}{Min}\left(X^T \boldsymbol{B}(Z)^T \boldsymbol{B}(Z) X\right) \quad (29)$$

This unconstraint optimization problem can be solved by mathematical software tool and then the angular parameters can be obtained.

After that, the distance among sensors can be computed from (27) if D_{12} is known as mentioned in previous section. It is also likely to calibrate D_{12} if an external angular measurement is available. To see this, substituting (27) into (4), we have,

$$\Delta\theta_{ij} = \frac{\sqrt{l_i^2 + l_j^2 - 2\cos(\gamma_{ij}) l_i l_j}}{D_{12} G_{ij}} sign(l_j \sin(\alpha_j + \sigma_{ij}) - l_i \sin(\alpha_i + \sigma_{ij}))$$

All l_i and l_j above can be determined from the same data set X. Define a new variable u as,

$$u = \frac{2}{N(N-1)} \sum_{i=1}^{N-1} \sum_{j=i+1}^{N} \left(\frac{\sqrt{l_i^2 + l_j^2 - 2\cos(\gamma_{ij}) l_i l_j}}{G_{ij}} \cdot sign(l_j \sin(\alpha_j + \sigma_{ij}) - l_i \sin(\alpha_i + \sigma_{ij})) \right) \quad (30)$$

As the result, the product of u and inverse of D_{12} is equal to average of the orientation estimation of each sensor pair. More precisely,

$$u \cdot D_{12}^{-1} = \frac{2}{N(N-1)} \sum_{i=1}^{N-1} \sum_{j=i+1}^{N} \Delta\theta_{ij} = \Delta\theta_{real} \quad (31)$$

where $\Delta\theta_{real,k}$ denotes the real rotation angle at each sample. Finally, the distance D_{12} can be directly obtained as

$$D_{12} = {}^{1}\!/\!_{u \cdot \theta_{real}} \tag{32}$$

V. Consistency Check Strategy

The performance of optical flow sensor depends on the condition of sensing surface. Highly reflective surface or a sudden change of height might disturb the sensor measurements seriously. Each pair of sensors can get a estimation of position and orientation according to (1) to (11), For N sensors, there will be $N(N\text{-}1)/2$ estimates. In order to reduce the uncertainty caused by the non-systematic error, the unreliable sensor measurements shall be removed from the update. The remaining measurements can used to update the position and orientation of the robot as described previously in (12) and (13).

From (18), if there is no error in the sensor measurements, $\boldsymbol{\varepsilon}$ should be zero. This means that the correct measurement vector X should lie in the null space of the matrix $\mathbf{B}$ (denoted as $\boldsymbol{N}(\mathbf{B})$). Therefore, for any vector X not in $\boldsymbol{N}(\mathbf{B})$, the orthogonal projection of X onto $\boldsymbol{N}(\mathbf{B})$ can be interpreted as the optimal correction of X. Alternatively, the distance of X to $\boldsymbol{N}(\mathbf{B})$ (or the error vector after projection) represents degree of incorrectness of the measurements. It is then possible to use this distance to access the reliability of each sensor measurement. Accordingly, there could be different kinds of strategies to access the reliability. For example, if one of the sensors gives an incorrect reading, we can find it out by removing it from X and the remaining sub-vector should be in the null space. Suppose the total number of unreliable sensors moved every time is Q. The measurement vector at time t is denoted as X_t. The procedure of finding out these Q sensors at each time that data coming is defined as following steps:

1) At beginning, the total number of sensors of X_t is N.
2) Ignore the measurements of one of these sensors and redefine a measurement vector, $X_{r,t}$, of remained sensors.
3) Find the constraint matrix, $\mathbf{B}_r$, of remained sensors and the null space of $\mathbf{B}_r$, $\boldsymbol{N}(\mathbf{B}_r)$
4) Find the orthogonal projection vector $\hat{X}_{r,t}$ of $X_{r,t}$ onto $\boldsymbol{N}(\mathbf{B}_r)$.
5) Calculate the distance from $X_{r,t}$ to $\hat{X}_{r,t}$
6) Repeat step 2 to step 5 until each sensor have been ignored once. Then compare all of distances that are collected in step 5 and find the minimum one.
7) Remove the sensor that was ignored corresponding to minimum distance in step 6. If the total number of removed sensors is equal to Q, then stop. Else, go to step 2.

After these steps, we can obtain the $(N-Q)$ reliable sensors at time t. And $\hat{X}_{r,t}$ can be used as the data set to compute the movement according to (1) – (11) and estimate the overall position and orientation by computing the mean of these movements as (12) and (13).

VI. Experimental Results

A module with eight optical flow sensors was developed as Fig.5. The optical flow sensor used is the ADNS-6010 type manufactured by Avago Technologies. This laser type sensor is better than the common optical ones since it is more accurate, less sensitive to height, and capable of measurement of higher speed motion. These 8 sensors are located at the corners of an octagon. The diagonal distance of the octagon is 4.8cm, and the relative orientation between two adjoining sensors is 45 degrees. The position and orientation of each sensor are held as precise as possible. The module contains a microprocessor which can access data of all sensors at the same time and send the data to PC through RS-232 in each sample time.

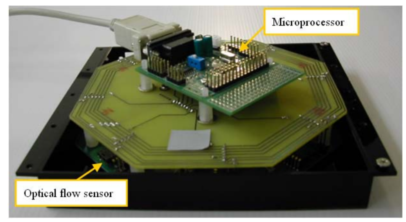

(a) Overall view

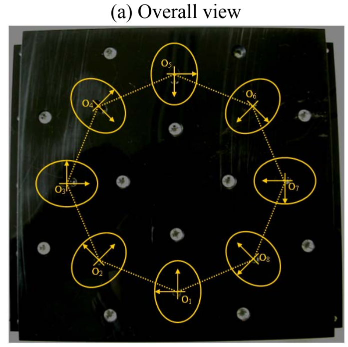

(b) Bottom view

Fig. 5.The module with eight optical flow sensors

In order to interpret clearly the effectiveness of the calibration method, random errors with a variance of 0.01 are added to the angles and the position of each sensor to represent the uncertainty of hardware installation. Firstly, we fixed a marginal point of the module and move the module spherically centered on that point. The sensing data are accumulated through a complete circle (radius 140 mm).

Then the accumulated data is used to formulate the optimization problem as (29). We use a built-in function named *fminunc* in MATLAB to solve this unconstraint optimization problem. Once angular parameters are obtained, the same accumulated data with actual 2π orientation is used to calculate the distance D_{12}. After that, experiment made by traveling the sensor module along the same circle again is performed comparing the estimation with nominal arguments and the estimation with calibrated arguments as in Fig. 6. Table I shows the detail of errors of the comparison.

Once again, let the robot move on the same path. But this time we put a piece of rectangular transparency at the midway to validate the consistency check strategy. The number of unreliable sensors moved every time is set to be 3. As shown in Fig. 7, the trajectory which doesn't implement the consistency check strategy has a sudden change when passing the transparency and results in a large error. In contrast, the one using the strategy as described in Section V successfully eliminates the faulty sensors and gives more accurate estimations. The detail of errors of returning to the end point is show in Table II.

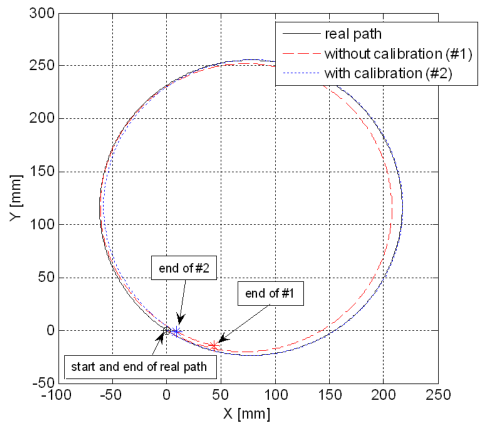

Fig. 6. The comparison of localization result with and without using calibrated arguments

TABLE I
ERRORS OF THE RESULT WITH AND WITHOUT CALIBRATION

	Position error		Orientation error	
	mm	%	degree	%
Without calibration	46.21	5.27	18.93	5.26
With calibration	8.60	0.98	2.72	0.75

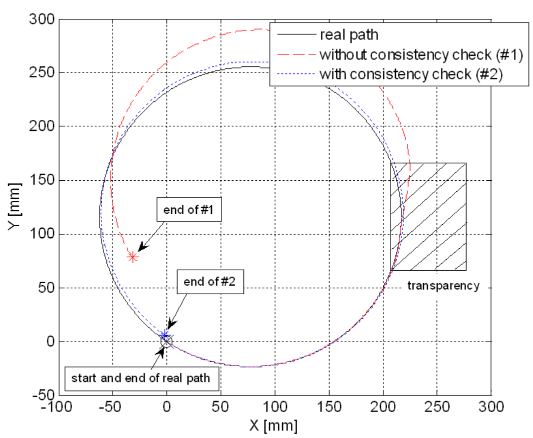

Fig. 7. The comparison of localization result with and without using consistency check strategy

TABLE II
ERRORS OF THE RESULT WITH AND WITHOUT CONSISTENCY CHECK

	Position error		Orientation error	
	mm	%	degree	%
Without consistency check	84.68	9.66	-24.95	6.93
With consistency check	6.28	0.72	-1.83	0.51

VII. CONCLUSION

In this work, an odometer using multiple optical flow sensors is introduced. Since the relative positions of the sensors are unchanged, their measurements should obey the rigid body constraint, i.e., the projections of velocity measurements of a pair of sensors onto the line connecting them should be the same. This relation is used first to calibrate the parameters of sensor configuration. It is shown that all parameters can be computed from the sensor measurements and the rotation angle of the module. To filter out incorrect sensor data during operation, the rigid body constraint is again used to construct the null space where sensor data vector should belong to. The reliability of the sensor data is determined based on the distance to the null space. Experiments are conducted to support the proposed methods and the results show the effectiveness of the methods in achieving a better accuracy.

REFERENCES

[1] J. Borenstein, H. R. Everett, and L. Feng, *Navigating Mobile Robots: Sensors and Techniques*, Wellesley, MA: A.K. Peters, 1996.

[2] J. Borenstein and L. Feng, "Measurement and Correction of Systematic Odometry Errors in Mobile Robots," *IEEE Trans. Robotics and Automation*, vol. 12, issue 6, pp. 869-880, Dec. 1996.

[3] D. K. Sorensen, "On-Line Optical Flow Feedback for Mobile Robot Localization / Navigation," *Texas A&M University*, Master Thesis, May 2003.

[4] S. Lee and J.B. Song, "Robust mobile robot localization using optical flow sensors and encoders," *IEEE Int. Conf. Robotics and Automation*, pp.1039-1044, Apr. 2004

[5] S. Lee, "Mobile Robot Localization using Optical Mice," *IEEE Int. Conf. Robotics, Automation and Mechatronics*, vol. 2, pp.1192-1197, Dec. 2004

[6] D. Sekimori and F. Miyazaki, "Self-Localization for Indoor Mobile Robots Based on Optical Mouse Sensor Values and Simple Global Camera Information," *IEEE Int. Conf. Robotics and Biomimetics*, pp. 605-610, 2005.

[7] A. Bonarini, M. Matteucci, and M. Restelli "Automatic Error Detection and Reduction for an Odometric Sensor based on Two Optical Mice," *IEEE Int. Conf. Robotics and Automation*, pp.1675-1680, Apr. 2005

[8] A. Bonarini, M. Matteucci, and M. Restelli "A Kinematic-independent Dead-reckoning Sensor for Indoor Mobile Robotic," *IEEE/RSJ Int. Conf. Intelligent Robots and Systems*, vol. 4, pp.3750-3755, 28 Sept.-2 Oct. 2005.

[9] J. Palacin, , I. Valgañon and R. Pernia, "The optical mouse for indoor mobile robot odometry measurement," *Sensors and Actuators A: Physical*, Volume 126, Issue 1, 26 January 2006, Pages 141-147

[10] J.-S. Hu, J.-H. Cheng, and Y.-J. Chang, "Spatial Trajectory Tracking Control of Omni-directional Wheeled Robot Using Optical Flow Sensors," *1st IEEE Multi-conference on Systems and Control (MSC)*, Singapore, October 1-3, 2007.

[11] J.-S. Hu, Y.-J. Chang, W.-H. Liu, and C.-H. Yang, "Localization of an Omni-directional Robot Platform Using Sound Field Characteristics and Optical Flow Sensing," *13th International Conference on Advanced Robotics (ICAR 2007)*, Aug. 21-24, 2007, Jeju, Korea.

[12] G. B. Gordon, D. L. Knee, R. Badyal, and J. T. Hartlove, "Proximity detector for a seeing eye mouse," United States Patent No. 6281882, Aug. 28, 2001